

Micropatterned surface electrode for massive selective stimulation of intraepidermal nociceptive fibres.

Massimo Leandri^{a,b}

Lucio Marinelli^{a,b,c}

Antonio Siri^{d,e}

Luca Pellegrino^e

- a) Department of Neuroscience, Rehabilitation, Ophthalmology, Genetics, Maternal and Child Health (DINOEMI), University of Genova, L.go Daneo 3, 16132 Genova, Italy
- b) Interuniversity Centre for Pain Neurophysiology (CIND), University of Genova, Via Dodecaneso 35, 16146 Genova, Italy
- c) Department of Neuroscience, Ospedale Policlinico San Martino, L.go R. Benzi 10, 16132 Genova, Italy
- d) Physics Department, University of Genova, Via Dodecaneso 33, 16146 Genova, Italy
- e) National Research Council. CNR-SPIN, Corso Perrone 24, Genova, 16152, Italy

Corresponding author:

Massimo Leandri.

Department of Neuroscience, Rehabilitation, Ophthalmology, Genetics, Maternal and Child Health (DINOEMI), University of Genova
L.go Daneo, 3,
16132 Genova, Italy

Email: massimo.leandri@unige.it

Tel. +39-010-3537081

The article has been published as: Leandri M, Marinelli L, Siri A, Pellegrino L. Micropatterned surface electrode for massive selective stimulation of intraepidermal nociceptive fibres. Journal of Neuroscience Methods 293C (2018) pp. 17-26. doi: 10.1016/j.jneumeth.2017.08.032. PubMed PMID: 28899650.

Abstract

Background

No satisfactory neurophysiological test for nociceptive afferents is available to date. Laser stimuli present risks of skin damage, whilst electrical stimulation through specially designed electrodes is not selective enough.

New Method

We present a new electrode designed according to critical issues identified in preliminary computer simulations concerning electric field gradient through the skin. To provide selective stimulation the activating electric field must be limited to intraepidermal free nerve endings. To this end, a new interdigitated electrode (IDE) was made of conductive rails arranged in a comb-like micropattern, situated only 150 μm apart from each other (150 IDE) and alternately connected to the opposite poles of the stimulator.

Results

Evoked potentials recorded from the scalp were obtained after stimulation with the 150 IDE and with a similarly designed, but more widely spaced electrode (1000 μm , or 1000 IDE). Small amplitude early and medium latency components were recorded with the 1000 IDE, suggesting activation of A β fibres. On the other hand, the 150 IDE only evoked late responses, confirming sufficient selectivity in small fibre activation.

Comparison with existing method(s).

The main differences with existing electrodes are:

- 1) Microspaced interdigitated conductive rails.
- 2) The potentially unlimited surface of stimulation and high efficiency per surface unit, resulting in large numbers of activated nociceptors.

Conclusions

A new electrode providing selective stimulation of nociceptive nerve free endings is presented. It is non-invasive, and its surface can be enlarged at will. It is expected that it may greatly help in neurophysiological assessment of conditions affecting the nociceptive pathway.

Keywords

Pain

Free nerve endings

Electrode

Micropattern

Evoked potentials

Stimulation

Acronyms

150 IDE (150 μm interdigitated electrode)

1000 IDE (1000 μm interdigitated electrode)

LEP (laser evoked potential)

PREP (pain related evoked potential)

SEP (somatosensory evoked potential)

1 Introduction

One of the mainstays of clinical electrophysiology is the ability to record activity of the nervous system evoked by suitable stimuli delivered to peripheral nerves or receptors. Refinements of hardware and software have brought important advances in detecting very small signals, even when embedded within undesired noise, provided that stimulus synchronization is feasible. Most of the techniques used so far allow objective and very reliable assessment of the nervous transmission, completely independent from the subject's alertness.

Unfortunately, such highly sophisticated tests are only suitable to explore the fast conducting fibres. So far, no electrophysiological method allows similar precision nor independence from the subject's collaboration when the transmission through small myelinated (A δ) or unmyelinated (C) fibres is concerned.

Two challenges are to be overcome. First, the selective stimulation of these two groups of fibres. Second, the recording of action potentials that are thousands of times smaller than those of the large fibres (unless they are "amplified" by the associative areas of the cortex, but this is another story).

In this paper we address the first challenge, that is selective stimulation. The best method developed so far is an infrared laser pulse, irradiating thermal energy in a short period of time, from 5 to 50 ms, and absorbed by the superficial layer of the skin, where only the free nerve endings of A δ and C fibres are situated. Long latency evoked responses are thus recorded from the scalp, related to the stimulus (Treede et al., 2003). However, there are several drawbacks: the heat pulse damages the skin, so it can only be repeated a few times, and never on the same spot; the device is costly, and, because the irradiated spot has very limited area, only a few afferents can be excited. In addition, the selectivity of solid state lasers has been questioned, as their radiation penetrates deep enough to also activate non-nociceptive receptors and fibres (Leandri et al., 2006). A simpler, but even more debated method, is represented by electrical pulses delivered through electrodes designed so that the generated field would stay superficial enough (Katsarava et al., 2006; Inui and Kakigi, 2012).

Unfortunately, the performance of the electrodes so far proposed has been challenged by a number of experiments, questioning their selectivity (Perchet et al., 2012). The electric stimulus in principle has optimal characteristics of control, ease of generation and delivery, instantaneous propagation (so that a number of fibres or receptors can be depolarized at the same time) and ease of synchronization with recording devices. We thought that the properties of the electric stimulus could be exploited provided the stimulating electrode could be designed in a more sophisticated manner. We investigated the existing electrodes, tested them with computer simulations as to the generated electric field, and here propose a new electrode which according to our simulation and experimental tests generates electric fields superficial enough to be selective for free nerve endings and at the same time able to activate a large number of receptors.

2 Materials and methods

2.1 Computer simulation

Finite element analysis of the electrode performance was carried out using Comsol Multiphysics® 4.3b (electric currents module) with a Intel® Core™ i7-3820 CPU @3.6GHz equipped with 64 Gb of RAM.

We studied the static response of the electrode considering a pure resistive model of the human skin adapted from one previously proposed (Mørch et al., 2011). It consisted of 4 layers: stratum corneum (thickness 29 μm), epidermis (60 μm), dermis (1300 μm) and hypodermis (5000 μm) having different conductivity values (stratum corneum $\sigma = 5 \times 10^{-4}$ S/m, epidermis $\sigma_x = 0.95$ S/m $\sigma_y = 0.15$ S/m, dermis $\sigma_x = 2.57$ S/m $\sigma_z = 1.62$ S/m, hypodermis $\sigma = 2 \times 10^{-2}$ S/m). The conductivity of the stratum corneum was set to match the resistance of our 150 μm and 1000 μm interdigitated electrodes (see section 2.3) measured in real experimental conditions. The voltage polarization and the ground conditions were applied to cathode and anode line regions with same dimension as the electrodes and which rested on the upper boundaries of the stratum corneum. Continuity conditions for current were set in the inner boundaries (interfaces between the layers), while electric insulation

conditions were set for the external boundaries. Free triangular meshes were employed for all layers, with maximum and minimum element size of 5 μm and 0.2 μm and 10(x):1(y) aspect ratio (y-direction scale =10) for both the stratum corneum and epidermis layers. Free triangular meshes with 1:1 aspect ratio and predefined “extremely fine” conditions were used for the dermis and hypodermis layers.

2.2 Subjects

All recordings were performed on ten healthy volunteers, 8 males and 2 females, ranging in age from 24 to 35 years, from the medical personnel of the Department of Neuroscience. All of them gave informed consent for the procedure and data treatment. The procedures were totally non-harmful and the study was carried out in accordance with the Code of Ethics of the World Medical Association (Declaration of Helsinki) for experiments involving humans. The study had been approved by the local ethics committee.

2.3 Electrodes

Three types of stimulating electrodes were used in the real experiments: i) a micropatterned interdigitated electrode with inter-rail distance and rail width of 150 μm (from now on named 150 IDE) (Fig. 1, bottom left), which was intended to stimulate the intraepidermal free nerve endings only; ii) a micropatterned interdigitated electrode with inter-rail distance of 1000 μm and rail width of 150 μm (from now on named 1000 IDE) (Fig. 1, bottom right), intended to stimulate deeper intradermal nerve fibres and iii) traditional, self-adhesive electrodes for surface stimulation of peripheral nerves, which will be referred to as “classic electrodes” in the text to follow.

The 150 IDE is the main object of this paper. It was designed and built as a prototype by three of the authors (M. Leandri, L. Pellegrino and A. Siri). The invention has been registered as Italian Patent n. 1425199, also published as WO/2015/186087, joint property of the University of Genova and Italian National Research Council (CNR). The 150 IDE and the 1000 IDE used in the experiments were made under licence by Bionen (Florence, Italy). They were made of a glass epoxy

substrate with a micropattern of gold conductor rails which interdigitated in a double comb-like fashion. Each of the two “combs” was connected to one of the stimulator poles. The area covered by these electrodes was in either case 10 x 10 mm.

The classic electrodes were type SilveRest by Vermed (Buffalo, New York), with dimension of 25 x 22.86 mm.

2.4 Sites of stimulation

The 150 IDE and 1000 IDE were always applied to the hairy skin of the hand dorsum between the 1st and 2nd metacarpal bone of the non dominant side (Fig. 1). Hairy skin was chosen because it is richly innervated by AMH II nerve endings (Treede et al., 1995), the main target of our work. The skin was gently cleansed with cotton wool moistened with ethanol then left to dry. The procedure had the advantage of cleansing the surface and reducing possible perspiration. Deliberately, no gel was used, to avoid electric shorting of the electrode rails.

In three subjects, the median nerve was stimulated at the wrist with the classic electrodes, cathode proximal.

2.5 Electric stimuli

Electric pulses of 0.2 ms duration were always used. These were delivered either as single or in bursts of 3, 5, 8, 10, according to the experimental design (see Section 2.8). The period inside the burst was 1 ms, so that a burst of ten pulses, for example, had an overall duration of 10 ms.

We used a constant voltage stimulator (EbNeuro, Florence, Italy), while voltage and current applied to the electrode were monitored through a purpose built optical isolator and read on the screen of an oscilloscope (TDS2004C, Tektronix, Beaverton, Oregon). Measured with this method, the impedance of the 150 IDE usually varied between 3 and 5 kOhm, and that of the 1000 IDE was 7-10 kOhm. In order that a perception threshold could be reached with the 150 IDE, a voltage of no less than 40-50 V had to be delivered. At the same time, a minimum current of 2-5 mA was necessary. The rate of stimulation was varied according to the experiment, as detailed in Section 2.8. Stimulus strength was set at 1.1-1.2 times the sensory perception threshold. Since its very

threshold, perception was always a moderately painful, localized pricking sensation with the 150 IDE. When the 1000 IDE was used, the subject also perceived a pricking sensation, but together with an electric shock like sensation irradiating towards the 2nd finger. The perception threshold with the 1000 IDE was reached at 1-2 mA, with voltages ranging between 50 and 70 V. As before, the stimulus strength was set slightly above the perception threshold.

2.6 Recording sites

Responses were recorded from the Erb site and from the scalp derivations Cz-Au_c, and C3'/C4'-Fz. At the Erb site, two subdermal needle electrodes were placed along and just behind the clavicle of the stimulated side, with the distal electrode connected to the non inverting input of the differential amplifier, and the proximal one connected to the inverting input.

On the scalp, the “active” electrode was always connected to the non inverting input of the amplifier, whilst the reference was connected to the inverting input.

In order to make our traces comparable to those of the literature, a polarity reversal was performed by software, and in all our figures an upward deflection signifies a negative potential applied to the non inverting input.

2.7 Signal amplification and processing

Signals were amplified 100,000 times, with bandpass 0.1-2000 Hz, 2nd order Butterworth analogue filtering (LT Bioamplifiers by Vertigo, Genova, Italy). They were then sent to an analogue to digital converter (NI PCIe-6320, X Series Multifunction DAQ, 16 bit, 250 KS/s sampling rate by National Instruments, Austin, Texas). Dedicated software, based upon the graphic language LabView 2014® (National Instruments, Austin, Texas), acquired 20,000 samples for 1000 ms after each stimulus, thus providing a high definition recording with a dwell time of 0.05 ms. Each single response was stored onto hard disc and kept for off line averaging.

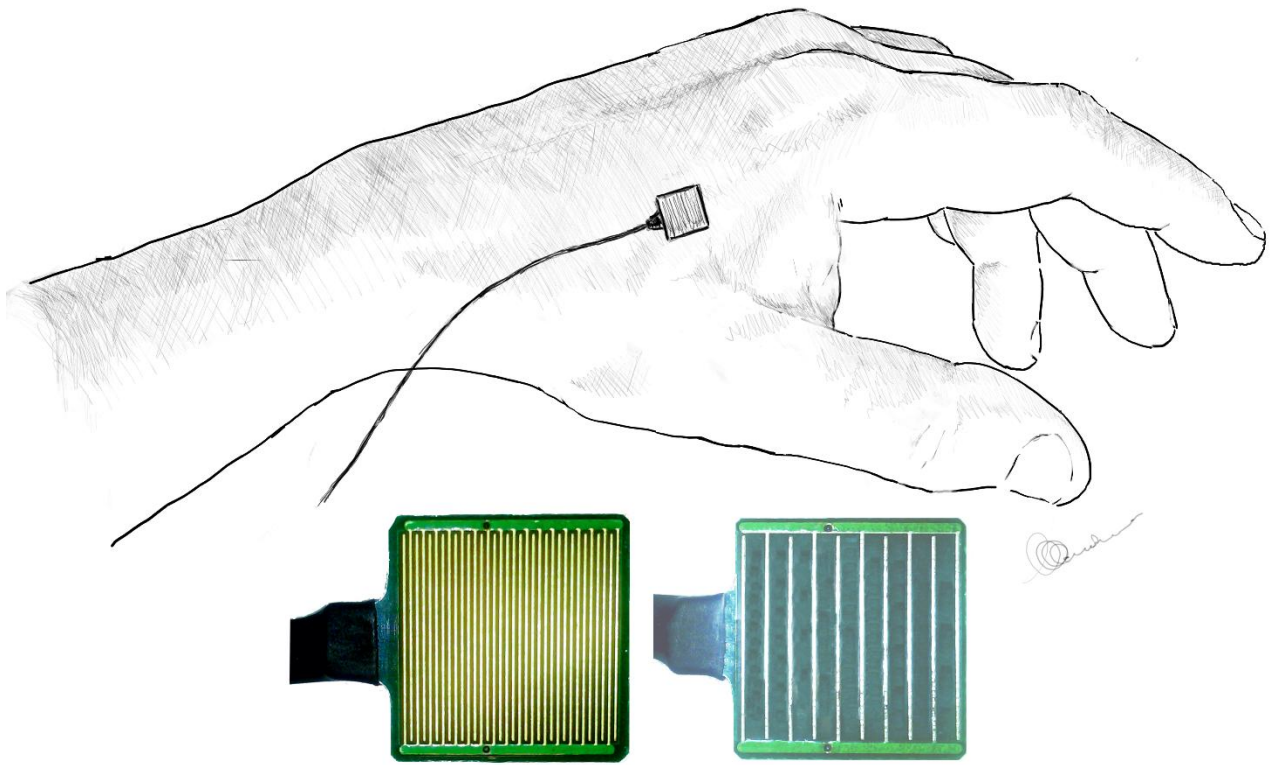


Fig. 1. Site of stimulation and electrodes.

Site of stimulation was on the skin between 1st and 2nd metacarpal bone. On the left is a photo of the 150 IDE, used to selectively activate the intraepidermal free nerve endings, and on the right the 1000 IDE which provided unselective activation of the cutaneous fibres.

2.8 Design of experiments

2.8.1 Set 1.

This was a preliminary set of experiments which was performed in 3 subjects, to check the response of peripheral nerve fibres to electric single pulses and to bursts (see 2.5 section for details). To do so, we used the median nerve, where the nerve trunk could easily be accessible at the wrist and high amplitude responses could be recorded at the Erb point (Fig. 5). Traditional bipolar stimulation with classic electrodes was used. Stimulation was performed at 1.5 times the intensity of the motor threshold for a thumb twitch, which ranged between 12 and 15 mA.

2.8.2 Set2.

The aim was to deliberately stimulate intraepidermal free nerve endings ($A\delta$ and C) and subepidermal $A\beta$ fibres of the hand dorsum skin, to compare early responses. Both 150 IDE and 1000 IDE were used, with repetitive fast stimulation (approximately 500 stimuli, with rate of 0.7/s). Recordings were performed from Erb point and C3'/C4'-Fz (Fig. 6 and Fig. 7). We used a burst of 5 pulses in order to allow recording of Erb point responses, which would have been hidden by the stimulus artefact with a longer burst.

2.8.3 Set 3.

This setting was aimed at stimulating the hand dorsum with 150 IDE electrode using random slow stimulation (20-30 stimuli with 10-20 s intervals) and recording from Cz-Au_c and C3'/C4'-Fz. Fig. 8). We asked the subjects to direct their attention towards the stimulus by counting the number of deliveries and by reporting changes in perception.

3 Results

3.1 Computer simulations of the electric field generated by our electrodes

All simulations were performed as 2 dimensional models, with the following parameters, according to the electrode types: i) 5.0 mm width and 6.389 mm height for the 150 IDE (Fig. 2a) and 1000IDE (Fig. 2b) micropatterned electrodes; ii) 10mm radius and 6.389 mm height for the axis-symmetric

model of the ring concentric electrode (Katsarava et al., 2006) (Fig. 2c); iii) 100mm width and 31.389 mm height for the classic electrode (Fig. 2d).

Fig. 2 shows the calculated distribution of the electric current for all three types of the experimental electrodes (the 150 IDE, the 1000 IDE, and the classic electrodes), plus the concentric electrode introduced by Katsarava et al. (Katsarava et al., 2006), that, although not tested in our experiments, was of interest in the simulations for comparison purposes. Calculations were performed on a 2D section of the electrodes as indicated in the figure. The alternated sequence of cathodic and anodic regions for the 150 IDE and 1000 IDE resulted in the electric current being distributed beneath the surface of the entire electrode, mainly in the stratum corneum and epidermis region. In the case of the circular electrode, the current was localized mainly under the central cathode, peaking at its edge.

The classic electrode (two SilveRest 25 x 22.86 mm placed in contact with the skin and 10 mm apart from each other) was modelled using a 2D model on a vertical cross section, as indicated in Fig. 2d, based on the same layered skin structure as that used for the micropatterned electrodes with the only exception of an increased width of the skin model (100 mm) and height of the hypodermis (30 mm). The electric current for the classic electrode yielded high values in the stratum corneum of the epidermis and also all over the dermis region between the anode and cathode, as shown in Fig. 2d.

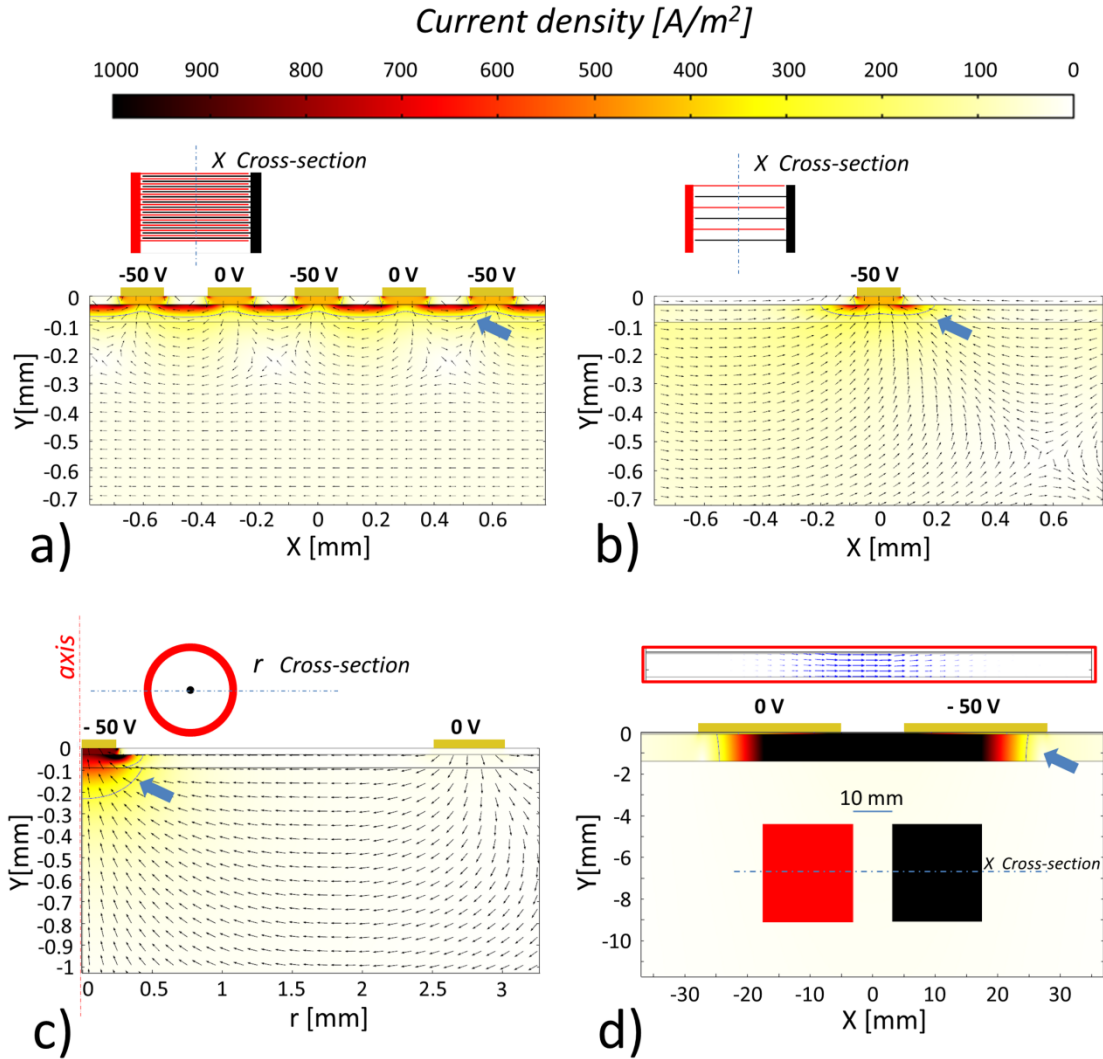


Fig. 2. Electric current under different electrodes. Calculated distribution of the electric current under the 150 IDE (a), 1000 IDE (b), concentric electrode (c) and classic electrode (d) is shown here. The colour plot represents the magnitude of the current density at the given electric polarization of -50 V applied to the cathodes. The arrow plot indicates flowing of the electrical current inside the skin. Length of arrows is normalized to the local current density magnitude (see also the colour plot for the associated magnitude) for (a),(b) and (c). The arrow plot of the classic electrode (d) is reported in the upper inlet, encased in red frame; arrow length is proportional to the magnitude of current density. The top view schematic of each electrode is also shown on each graph together with the line cross-section used for simulations. The blue contour lines (marked by the large blue arrow) indicate the spatial regions where the current density has the representative value of 250 A/m^2 . Colour scale saturates for values above 1000 A/m^2 , the maximum values of the current density being about 2170 A/m^2 for the 150 IDE, 2165 A/m^2 for the 1000 IDE, 4330 A/m^2 for the circular electrode and 3300 A/m^2 for the classic electrode.

In order to visualize the regions where excitation of the fibres would take place, we plotted the activating function, defined as the second spatial derivative of the extracellular potential along the axis of a nerve (Rattay, 1986; Grill, 1999) and which is used to evaluate the efficiency of an electrode by providing an indication of where the action potential preferentially will develop. As the nociceptive fibres are directed along the skin's depth, we considered the activating function along this direction (y) only. The magnitude of the applied voltage, and the consequent value of the activating function, is a free parameter during stimulation; for this reason the activating function has been normalized to its value taken at $-50\ \mu\text{m}$ under the skin surface below the center of each electrode's cathode.

As shown in Fig. 3a, the circular electrode (diameter of the inner conductor $0.5\ \text{mm}$) shows a peak of the activating function at its edge in a region length extending for about $100\ \mu\text{m}$ below the surface of the skin. It is worth noting that the diameter of the inner conductor does not significantly affect the actual stimulating area, because the higher values of the activating function are located at the borders, as already reported by other authors (Mørch et al., 2011)

In contrast to the concentric electrode, our 150 IDE yields a completely different pattern of the activating function. Firstly, its -3 contour line, as shown in Fig. 3b, only reaches a depth of approximately $-35\ \mu\text{m}$, about $1/3$ of the concentric electrode.

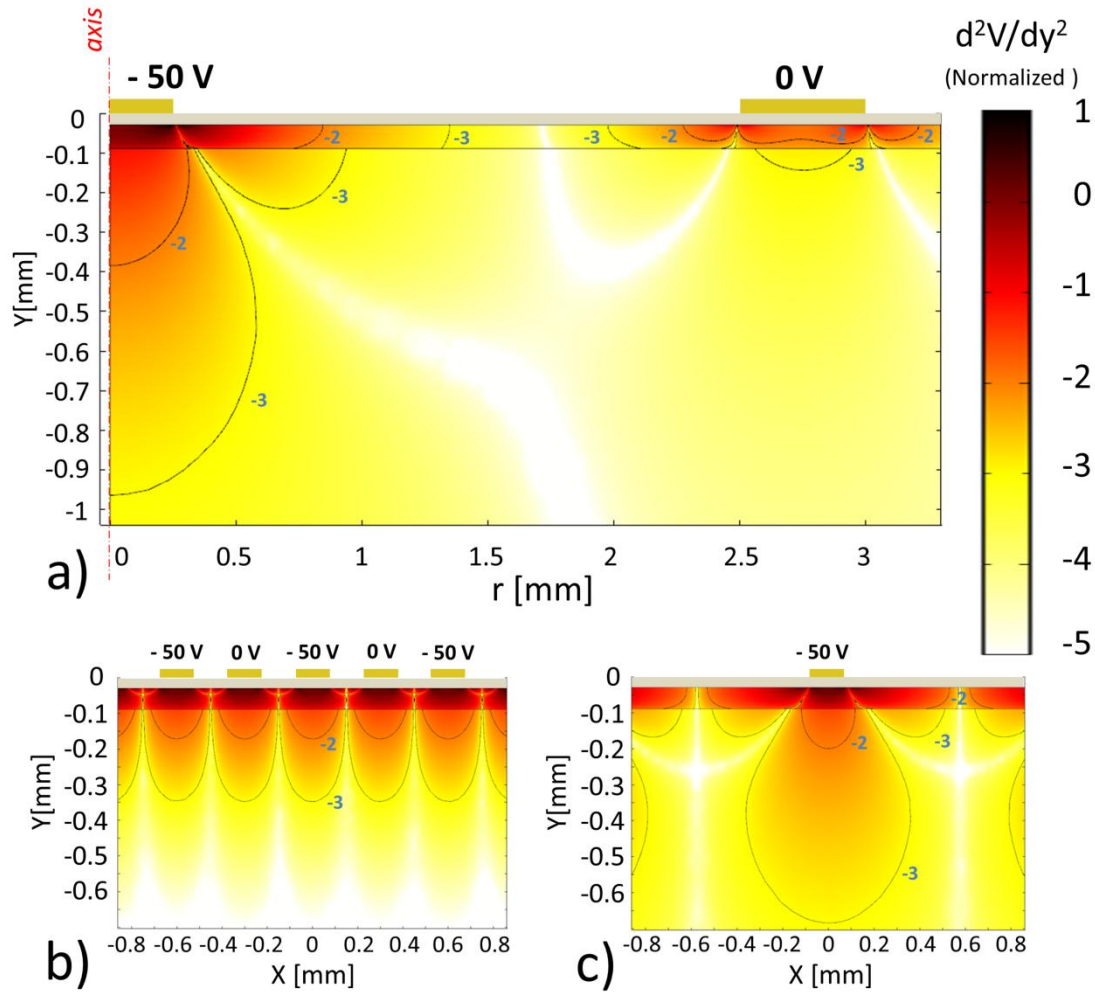


Fig. 3. Absolute value of the activating function for the concentric electrode (a), 150 IDE (b) and 1000 IDE (c).

The activating function is calculated along the vertical direction where free nerve endings are mainly oriented. The activating function has been normalized to its value taken under the centre of each cathode at $-50 \mu\text{m}$ depth, where its absolute value is $3.16 \times 10^7 \text{ V/m}^2$ for the concentric electrode, $3.91 \times 10^7 \text{ V/m}^2$ for the 150 IDE and $3.91 \times 10^7 \text{ V/m}^2$ for the 1000 IDE. The colour plot is in logarithmic scale. The black contour lines identify the spatial regions where the activating function is 100 (-2 numbers) and 1000 (-3 numbers) times lower than the normalized value (0 in the logarithmic scale). The maximum value taken by the logarithm of the activating function is 0.83 for the circular electrode, 0.47 for the 150 IDE and 0.51 for the 1000 IDE. The stratum corneum has been coloured grey to signify that no fibres are present in it.

Secondly, the activating function for the interdigitated electrode pattern and the associated regions of activation is periodically repeated for about 25% of the whole electrode area, calculated as the normalized ratio between the amount of cathode area and the whole electrode area. The same calculation results in a ratio of less than 1% for the ring concentric electrode. As shown in Fig. 3b

and c, the effect of the inter-rail gap in the interdigitated electrodes is to change the lateral distribution of the activating function below each rail, consequently affecting the stimulation area. A clear idea of the importance of the inter-rail gap as to the spatial distribution of the activating function can be gathered by examining the simulation related to the 1000 IDE. Here, the -3 contour plot reaches a depth of about 70 μm below skin surface, double that of the 150 IDE.

In the case of the classic electrode, the activating function only decreases by an order of magnitude (-1 contour plot) by the depth of about 9 mm, well below the epidermis layer (Fig. 4a). Such deep spread of the activating function is a clear indication that the classic electrodes yield a much smoother distribution of the generated field than the interdigitated micropatterned electrodes, with uniform penetration of the skin and subcutaneous, reaching suitable values to activate low threshold deep myelinated fibres, without necessarily depolarizing the high threshold superficial free nerve endings. Similarly to the other electrodes, the activating function is peaked at the electrode borders (Fig. 4b and Fig. 4c), but the small area of these border regions and the large gap between anode to cathode (here 10 mm) prevents efficient and selective stimulation of unmyelinated fibres.

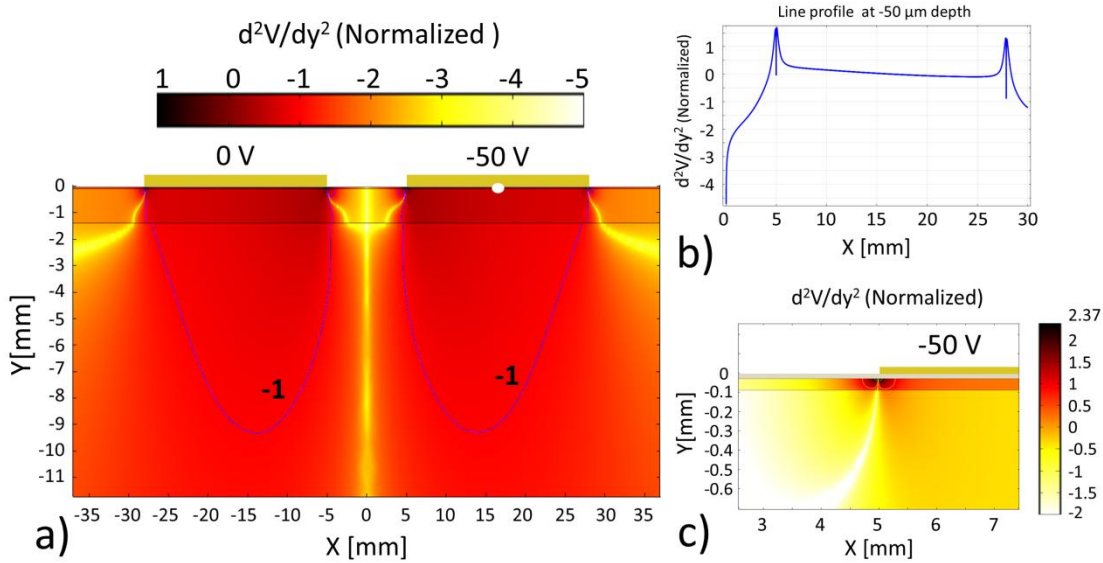


Fig. 4. Absolute value of the activating function for the classic electrode.

In (a) the surface colour plot of the activating function is shown, normalized to its absolute value ($3 \times 10^5 \text{ V/m}^2$ taken below the centre of the cathode at $-50 \mu\text{m}$ depth (white dot)). In all plots the normalized values of the activating function are reported in logarithmic scale. The blue contour lines indicate those regions where the activating function is 10 times lower (-1 value) than the normalized value. The activating function peaks at the electrode edges, as is evident in its line profile normalized at $-50 \mu\text{m}$ depth (b) and in the zoomed image (c) where it reaches its maximum value just below the edges (230 times the normalized value).

Summing up, the finite element model of Fig. 3 showed that high values of the activating function were achieved in the epidermis layer for all three electrodes, but the 1000 IDE and the circular electrode still showed a comparatively high value (approximately 10^4 V/m^2) of the activating function reaching well into the dermis at the respective depths of about 0.7 mm and 0.95 mm. On the other hand, the 150 IDE showed a steeper decrease of the activating function, with the same value of 10^4 V/m^2 being reached at the depth of about $-350 \mu\text{m}$. These results predict that the 1000 IDE and the circular electrode should stimulate also the deeper fibres ($A\beta$) of the dermis and should not be considered selective for the $A\delta$ fibres. As an aside observation, it is worth noting that the 150 IDE needs a lower value of the applied potential (and lower electric field in the stratum corneum) to achieve the same value for the activating function as the 1000 IDE at the normalization point situated $-50 \mu\text{m}$ below the cathode, thus minimizing the nonlinear effects of the electric field inside the skin. The distribution of the values of the activating function along the skin depth depends also

on the values of the conductivity of each layer and their reciprocal ratio (the potential drop is divided by the layers) as well on their anisotropy. Stimulation efficiency and selectivity of each electrode may be modified if changes in the induced electric field take place following variations in tissue conductivities during stimulation, as may happen where electroporation takes place. For this reason, monitoring current and voltage during stimulation with any electrode, in order to assess impedance, would be strongly advisable.

3.2 Results of experiments

3.2.1 Response of A β fibres to bursts

Stimulation of the median nerve trunk at the wrist was solely performed to check whether the myelinated large fibres (A β) would respond to single pulses and to high frequency bursts. As we were going to use a burst of pulses in order to activate at the lowest possible threshold the intraepidermal thin fibres, it was also important to know how the A β fast fibres would respond to this sort of stimulus. In fact, the response of A β fibres (or the lack of it) was later used in our experiments to assess the selectivity of our device and method of stimulation. Recordings of the activity from the Erb point in response to stimuli either single or in burst are shown in Fig. 5. No relevant change in the Erb response could be detected when different modalities of stimulus were used. We consider this to be evidence that A β fibres responded to the first pulse only, as obviously the fibres were in the refractory period when the following pulses were delivered. It could then be safely assumed that delivering a burst of n pulses with interpulse less or equal to 1 ms would give rise to no further responses due to subsequent activation of the large peripheral axons anywhere in the peripheral or central nervous system. Whatever changes in responses might occur when changing the number of pulses, these would be due to something not related to multiple activation of A δ fibres in the course of time.

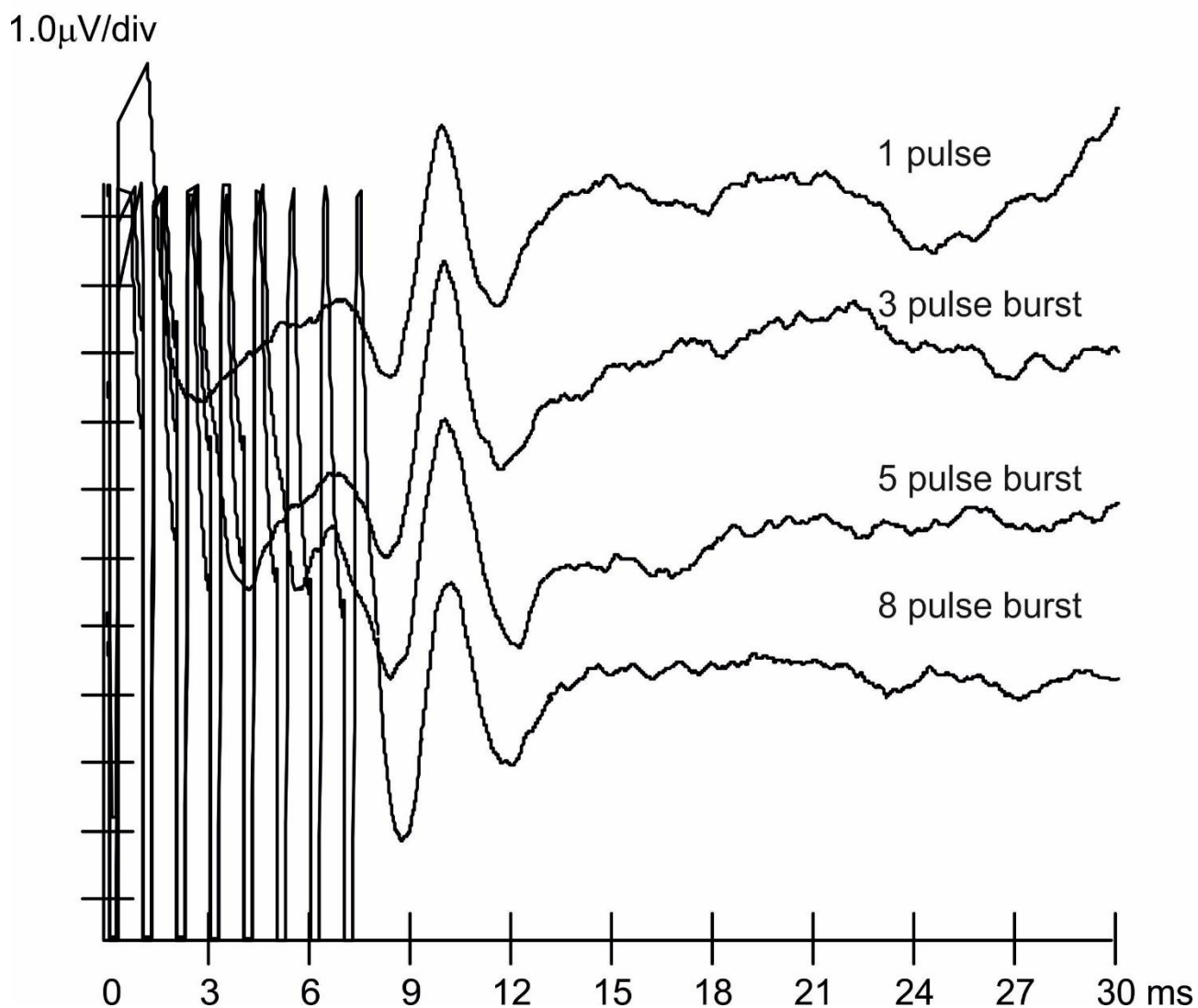


Fig. 5. Erb responses to stimulation of the median nerve trunk at the wrist. This is to show that the peripheral nerve response (fast fibres recorded at Erb site) is only linked to the first pulse of a burst. The Erb potential of the bottom trace is distorted by the stimulus artefact. Negativity in this and other figures is upwards.

3.2.2 Evoked potentials after A β stimulation of the hand dorsum skin.

Compound action potentials recorded from the Erb site and from the scalp (C3'/C4'-Fz) after stimulation of the hand dorsum skin with the 1000 IDE are shown in Fig. 6. The aim of this experiment was to demonstrate that the activity of A β afferents from this site (the same site that will later be used for selective stimulation of A δ fibres with the 150 IDE) could be recorded as SEPs. In order to average a sufficient number of responses (approximately 500), repetitive stimuli at the rate of 0.7/s were delivered. A small negative response could be recorded at the Erb site with latency of 10.6 ± 0.7 ms, and amplitude (from baseline to negative peak) of 0.92 ± 0.48 μ V. From C4'-Fz a small negative-positive component could be observed (marked as N20 in Fig. 6 because of its reputed similarity to the median nerve SEP component) with peak latencies of 23.7 ± 1.8 ms (amplitude from baseline 0.38 ± 0.24 μ V) and 26.4 ± 2.5 ms (interpeak amplitude 0.82 ± 0.36 μ V). It was followed by a second, larger negative-positive wave, peaking at 27.7 ± 2.2 ms and at 32.9 ± 2.61 ms (interpeak amplitude 3.8 ± 1.8 μ V). The general shape and latencies of these components resembled the classic W shape that can be observed in traditional recordings of somatosensory evoked potentials (SEPs) from the C4'/C3'-Fz derivations after stimulation of the upper limb.

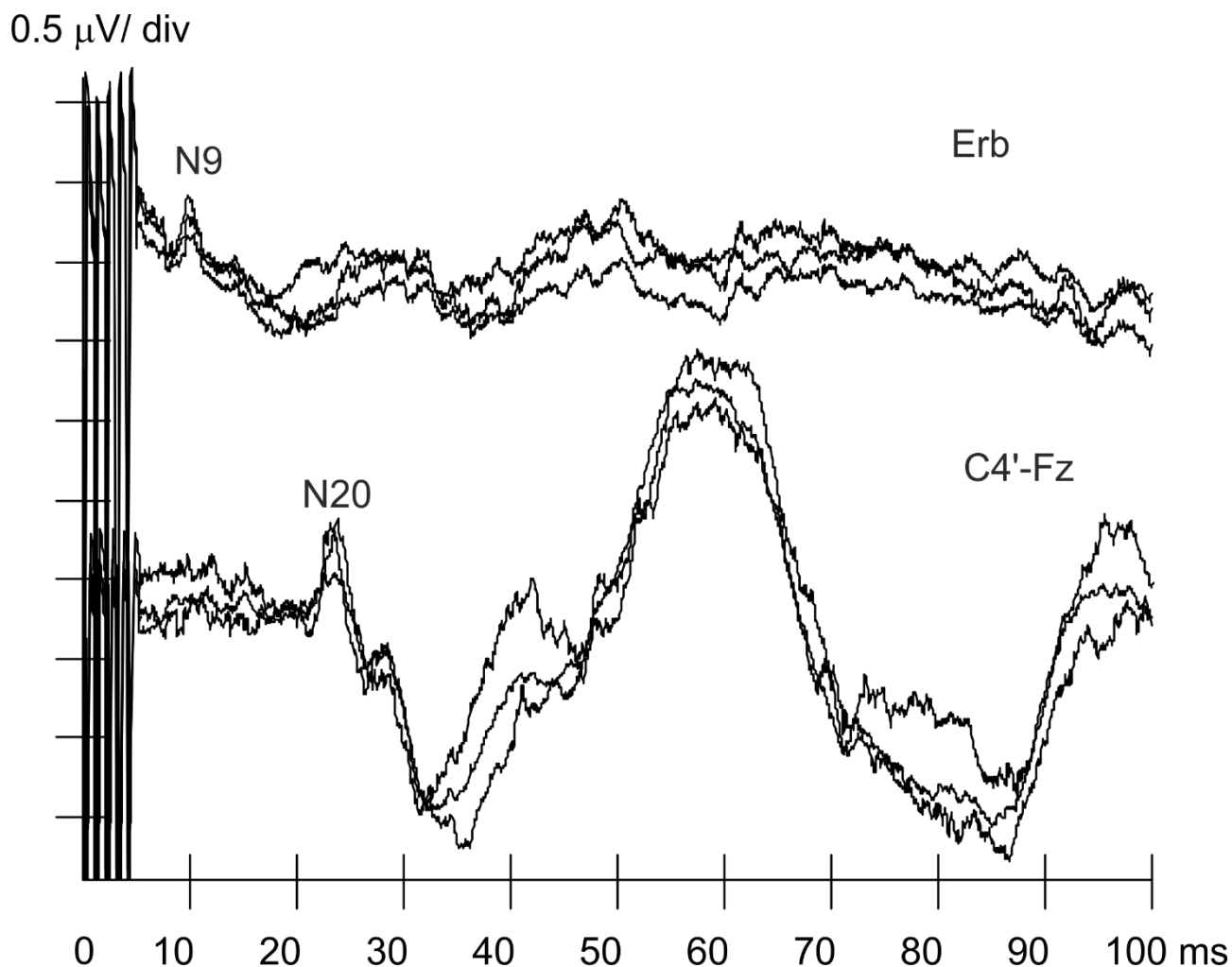


Fig. 6. 1000 IDE on hand dorsum, with 5 pulse burst.
 This is to show that stimulation of cutaneous large afferent fibres with 1000 IDE gives rise to recordable, though very small, responses at the Erb point and to early/medium latency cortical responses.

3.2.3 Scalp evoked potentials after repetitive stimulation with 1000 IDE and 150 IDE.

With this experiment we compared the effect of stimulation with 1000 IDE versus 150 IDE on responses from the sensorimotor primary area (Fig. 7), by using bursts of 10 pulses, delivered at constant repetition rate of 0.7/s. The aim of the experiment was to demonstrate that while the 1000 IDE would evoke early SEP components as already described in paragraph 3.3.2, the use of 150 IDE would not. Our recordings confirmed this hypothesis, as can be seen in the lower set of traces of Fig. 7 depicting the response to 1000 IDE, where the early and medium latency typical SEP components are clearly shown (only N20 is labelled here), albeit with very small amplitude.

Conversely, the only responses obtained from the 150 IDE are in the late range, the first of them a negative peak at the mean latency of 91.4 ± 12.0 ms, similar to the well known LEP or PREP N1. Its amplitude was 2.4 ± 1.5 μ V, well below the usual amplitude of LEPs (Treede et al., 2003) and PREPs (Katsarava et al., 2006; Perchet et al., 2012). The reason for such behaviour is very likely to be found in the rate of stimulation, which was too fast and constant to be able to elicit large late components.

It can be observed that a similar late wave is recorded after stimulation with the 1000 IDE (lower traces of Fig. 7), marked as SEP N1. Such a component could not be seen in our previous C4'-Fz recordings with 5 pulse burst shown in Fig. 6 (lower traces), probably because the combination of high repetition rate and shorter burst did not reach the necessary perceptual significance.

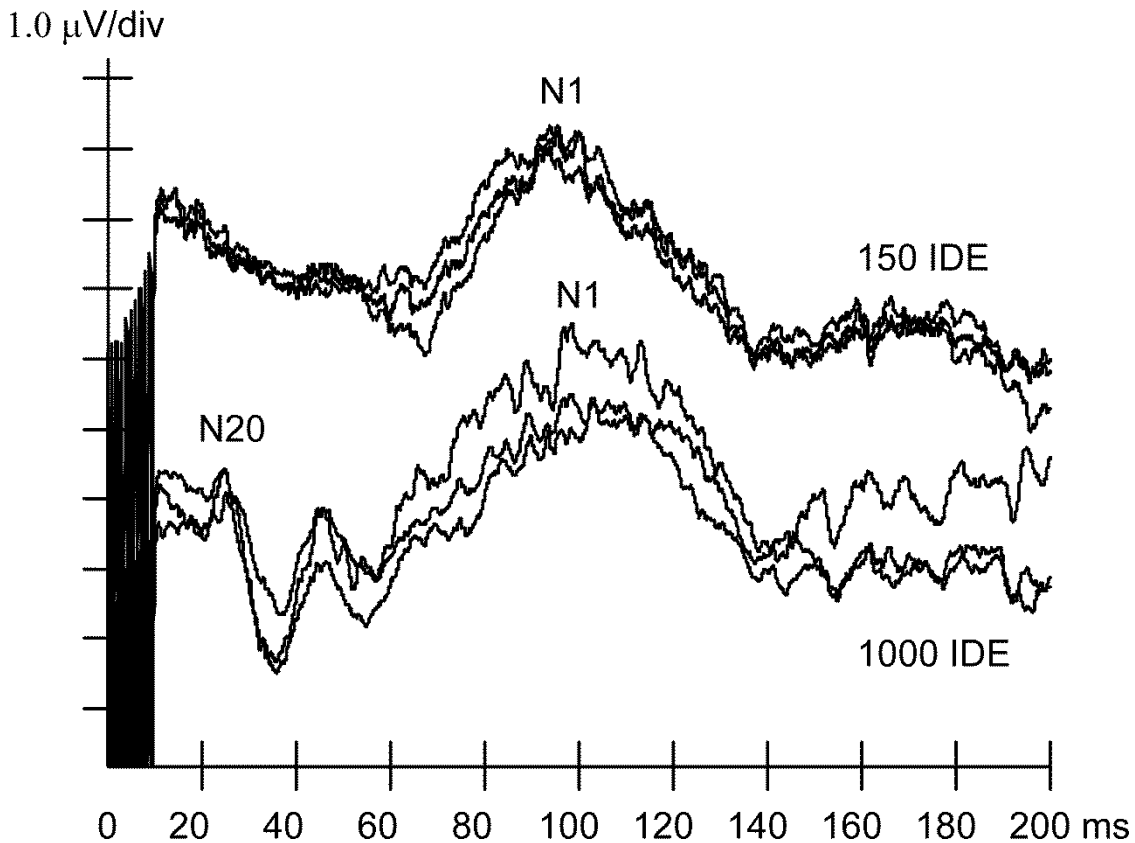


Fig. 7. Cortical evoked potentials after fast stimulation rate. Recordings from C4'-Fz derivation after fast, repetitive stimulation with 150 IDE (upper traces) and 1000 IDE (lower traces) electrodes are shown here. The lower traces show early/medium latency waves preceding the late component seen at 100ms. The upper traces only show a late wave peaking at 100ms.

3.2.4 Scalp evoked potentials after random stimulation with 150 IDE

Large late responses were recorded at Cz-Au_c and C3'/C4'-Fz, similar to those seen in LEPs and PREPs, but no early components could be seen (Fig. 8). From Cz-Au_c derivation, the first reliable wave that could be seen had positive polarity, with mean latency of 89.7 ± 17.2 ms, and amplitude of 8.7 ± 2.8 μV as measured from baseline. It was followed by a larger, negative peak at 122.4 ± 11.5 ms (labelled N1) and a positive peak at 175.4 ± 23.7 ms (labelled P2). Peak to peak amplitude of the latter complex was 35.8 ± 9.6 μV. Derivation C3'/C4'-Fz yielded a first negative peak at mean latency of 75.7 ± 13.8 ms (labelled N1) and amplitude from baseline of 13.2 ± 6.3 μV. A

much larger negative peak at 105.8 ± 13.8 ms (labelled N2) and a positive one at 162.6 ± 25.6 ms (labelled P2) followed on, with interpeak amplitude of 41.5 ± 18.7 μ V.

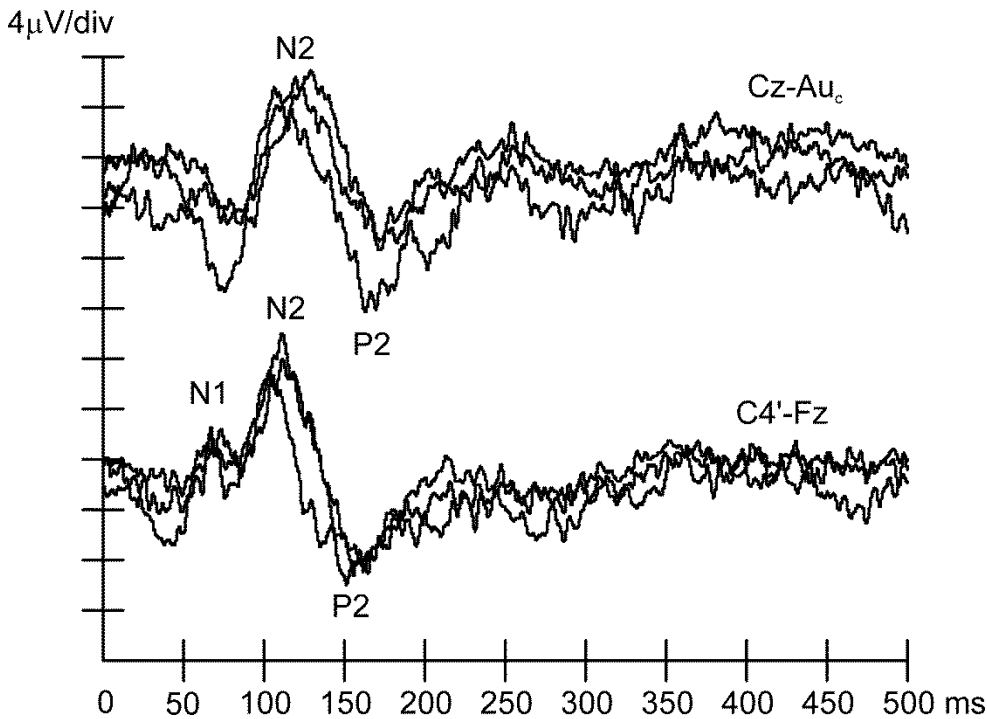


Fig. 8. Cortical evoked potentials after random stimulation with 150 IDE. Average of 20 responses per trace. Painful perception was graded 4-5. Stimulus artefact is not visible, as the traces have been processed off line with the LabView © Butterworth filter function, set as 1st order 0.1-500 Hz bandpass.

3.2.5. N1 in different conditions.

Among the late waves, N1 seems to be the most constantly recorded component in our experiments. It may be worthwhile to compare N1 latency and amplitude between responses obtained with 1000 and 150 IDE, the latter both in repetitive and random modality. Fig. 9 illustrates what can be found. When using repetitive stimulation, latency of N1 was significantly ($p = 0.015$) shorter in the case of 150 IDE than 1000 IDE, with a mean difference of 9.5 ms. But there was no significant amplitude difference between the two electrodes in this condition. A comparison between random slow stimulation versus repetitive fast stimulation, always using 150 IDE, shows that in the former

condition N1 occurred 15.6 ms earlier, but not significantly ($p = 0.18$). Its amplitude, on the other hand was far larger in slow random modality, with a very significant ($p = 0.00003$) difference of $10.9 \mu\text{V}$.

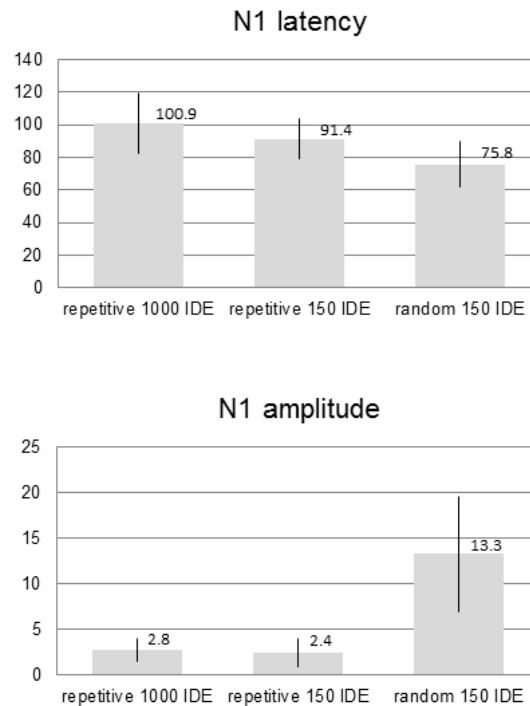


Fig.9. The N1 component.

This is to show latencies in ms and amplitudes in μV of the cortical component N1 recorded at C3'/C4'-Fz in various conditions of stimulation. Random slow stimulation yields a larger N1 than the fast repetitive modality, obviously suggesting that a quick habituation process takes place.

4 Discussion

4.1 Computer simulations and electrode design

In theory, selective activation of the nociceptive afferents by an electric field could be achieved by limiting its diffusion through the skin, so that the related activating function for unmyelinated fibres (Rattay, 1986) was sufficient to depolarize the thin fibres within 50-100 μm from the surface (i.e.

the epidermal layer, only populated by the unmyelinated free nerve endings), but would not significantly affect the deeply situated, large myelinated fibres. So, the circular electrode previously introduced by Katsarava et al. (Katsarava et al., 2006) might be suitable to elicit activity in the free nerve endings in a tiny region of the epidermis. But this effect could only take place at the electrode edges, as demonstrated by our simulation, where the number of activated fibres would be too small to evoke any recordable response. In order to recruit larger numbers of fibres the only option is to increase the stimulus strength, but this would result in a deeper spread of the electric field, together with the related activating function, and a consequent loss in selectivity. In fact, the concentric electrode has not been found to be selective enough when seeking cortical evoked responses (Perchet et al., 2012), but of course it has been hypothesized that at very small stimulus strengths sufficient selectivity could be accomplished (Mouraux et al., 2010). Analysis of computer simulations suggested that one primary objective should be the increase of edge covered area, so that a large number of free nerve endings are affected, without the need to increase stimulus strength. A further goal should be the reduction of distance between conductors linked to opposite poles, which could help in keeping the activating function as superficial as possible. The design of our 150 IDE meets these two needs as it is based upon a micropatterned modular unit that could be repeated as many times as needed to cover a given area, without altering the interconductor distance and therefore not affecting the field depth.

The electrode thus offers a practical solution to increase the number of borders, while maintaining at the same time a simple scheme for the electric connections.

4.2 The stimulus: burst of pulses

It is imperative that in order to limit the spread of the electric field we should use not only a suitable electrode geometry, like the proposed micropattern, but also keep the stimulus strength at a minimum, approaching as much as possible the threshold for A δ fibres. According to the strength duration curve, the minimum strength of stimulus needed to start an action potential is linked to the stimulus duration: the longer the stimulus the less the strength needed. However increasing duration

above a certain limit, does not bring any relevant decrease of the necessary stimulus strength. Although excitability thresholds vary considerably according to the experimental conditions, we know that chronaxie values for A δ fibres are in the range of 1ms (Mengel et al., 1993), and the time constant for the same group has been reported between 5 and 15 ms (Hodgkin, 1948). Therefore we thought that a duration of 10 ms could ensure the lowest possible strength needed to activate those fibres. Commercial stimulators usually do not deliver stimuli of such duration without heavy distortion of the square waveform, with unpredictable effect upon the excitable membrane. However, a train of short pulses could easily be delivered without distortion, and its overall effect could be the same as a single longer pulse, provided the inter-pulse period is kept short enough. The absolute refractory period of the large myelinated fibres is reported in a review to be approximately 0.5-1ms, and relative refractory period between 3 and 4 ms (Burke et al., 2001), so pulses following the first one at 1ms interval should not be able to generate an action potential even on the fastest fibres. Our recordings after stimulation of the median nerve were aimed at demonstrating such a hypothesis, which was duly confirmed.

4.3 The evoked potentials

It is noteworthy that the technique of late evoked potentials has usually been applied to pain research with no attention at all to early or medium latency components. This was due to the notion that pain afferents would be too slow and desynchronized to be recorded peripherally. At the same time the elicited cortical activity would be spread over wide areas of cortex involving a large number of synapses. So nothing could be expected to be seen before 80-100 ms after the stimulus. Whatever the technique, since the first attempts with tooth electrical stimulation, then laser heat pulses, and eventually fast contact heat devices, the resulting response has always been in the latency and spatial distribution range of the endogenous event related potentials and was strongly linked to attention (Oken, 1997). Investigations about PREPs after electric stimulation with concentric electrodes, either surface or intradermal, followed suit. Usually, the very settings of the recording system (number of averages, bandpass and sampling rate), when tuned to late responses,

prevent the recording of fast components. To our knowledge, no attempt has ever been made to assess whether early and medium components were present in the cortical evoked responses generated by electric stimulation via allegedly selective electrodes.

There is little doubt that, besides the many advantages of the electric pulses over caloric stimuli in activating the nerve endings, there is the possibility by the former of being delivered at high rates and for a long time without risk of tissue damage or modification of tissue background temperature. In our experiments such features were exploited in order to obtain very low noise averages, which showed low amplitude early and medium latency components, when using the 1000 IDE unselective electrode for stimulation. This approach had not been used before, and we consider it to be the most reliable non-invasive method so far used to provide evidence that the two types of electrodes (150 IDE and 1000 IDE) activate different populations of fibres.

The late components that we recorded from the scalp after stimulation with the 150 IDE were best seen when a slow, random rate of stimulus delivery was used. Latencies obtained by us in this modality were shorter than those described by other authors with lasers, but also shorter than those reported with electric stimulation through concentric electrodes. When comparing latencies and amplitudes of the late waves N1, N2 and P2, one should always keep in mind that these are cognitive potentials with a very high degree of inter- and intra-subject variability, and that the importance of attention is paramount (Iannetti et al., 2008). Their aspecific nature has long been known and they cannot be considered as an objective representation either of the qualitative or quantitative intrinsic properties of a stimulus (Mouraux and Iannetti, 2009). Furthermore, the comparisons shown in Fig. 9 about N1 support the idea that even in the same setting latencies and amplitudes may not be directly related to the type of activated fibres, but rather to modality of stimulation. For such reasons, it is no wonder that latencies detected in one laboratory may not perfectly overlap those found elsewhere and with different methods.

A comment over the cortical responses by C fibre stimulation is due here. Such long latency, ultra-late responses are best seen after temperature controlled laser stimulation (Magerl et al., 1999), and

are usually inhibited if A δ co-activation is performed. Whilst there is little doubt that the activating function arising from our stimuli could excite nerve free endings pertaining to A δ and C fibres, we had no chance to perform a selective stimulation of C fibre nerve endings. For this reason, no attempt was made to record ultra-late cortical responses (the 1000 ms epoch time after stimulus would have been too short to clearly visualize such responses). It is also important to note that the aim of our work was to demonstrate that the 150 IDE could selectively activate intraepidermal free endings and our efforts were focused on a neurophysiological demonstration of this feature versus unselective activation of A β fibres by 1000 IDE. This meant that an accurate analysis of early and middle latency responses had to be performed, leaving comparison between late and ultra-late responses to a future chapter of the research.

Despite their lack of objectivity, the late evoked potentials are so far the only available instrumental method to investigate pain afferents. On condition, of course, that the stimulus is of a nociceptive nature, and that no significant numbers of non nociceptive afferents are stimulated. We propose the 150 IDE as an instrument to achieve such selective stimulation.

5 Conclusions

In contrast to previous electrodes, with small stimulating surfaces but great distances between opposite poles, our electrode is characterized by a micropattern that can be repeated as many times as it is convenient, with tiny gaps between opposite poles. This design assures that the spread of electric field remains the same independently from the extent of stimulated area. At the same time, the estimate amount of activated intraepidermal free nerve endings, per surface unit, is 25 times that of other electrodes based upon concentric design. The scalp recorded evoked potentials demonstrated the selectivity and efficiency of our electrode, which we now believe will be suitable for practical and reliable use in laboratories of clinical neurophysiology.

6 Bibliography

- Burke, D., Kiernan, M.C., Bostock, H., 2001. Excitability of human axons *Clin. Neurophysiol* 112, 1575–1585.
- Grill, W.M., 1999. Modeling the effects of electric fields on nerve fibers: influence of tissue electrical properties. *IEEE Trans. Biomed. Eng.* 46, 918–928. doi:10.1109/10.184700
- Hodgkin, A.L., 1948. The local electric changes associated with repetitive action in a non-medullated axon. *J. Physiol.* 107, 165–181. doi:citeulike-article-id:2252626
- Iannetti, G.D., Hughes, N.P., Lee, M.C., Mouraux, A., 2008. Determinants of laser-evoked EEG Responses : Pain Perception or Stimulus Saliency ? 815–828. doi:10.1152/jn.00097.2008.
- Inui, K., Kakigi, R., 2012. Pain perception in humans: use of intraepidermal electrical stimulation. *J. Neurol. Neurosurg. Psychiatry* 83, 551–556. doi:10.1136/jnnp-2011-301484
- Katsarava, Z., Ayzenberg, I., Sack, F., Limmroth, V., Diener, H.C., Kaube, H., 2006. A novel method of eliciting pain-related potentials by transcutaneous electrical stimulation. *Headache* 46, 1511–1517. doi:10.1111/j.1526-4610.2006.00446.x
- Leandri, M., Saturno, M., Spadavecchia, L., Iannetti, G.D., Cruccu, G., Truini, a, 2006. Measurement of skin temperature after infrared laser stimulation. *Neurophysiol. Clin.* 36, 207–18. doi:10.1016/j.neucli.2006.08.004
- Magerl, W., Ali, Z., Ellrich, J., Meyer, R.A., Treede, R.D., 1999. C- and A delta-fiber components of heat-evoked cerebral potentials in healthy human subjects. *Pain* 82, 127–137.
- Mengel, M.K.C., Jyvasjarvi, E., Kniffki, K.-D., 1993. Identification and characterisation of afferent periodontal A δ fibres in the cat. *J. Physiol.* 464, 393–405.
- Mørch, C.D., Hennings, K., Andersen, O.K., 2011. Estimating nerve excitation thresholds to cutaneous electrical stimulation by finite element modeling combined with a stochastic branching nerve fiber model. *Med. Biol. Eng. Comput.* 49, 385–395. doi:10.1007/s11517-010-0725-8
- Mouraux, A., Iannetti, G.D., Plaghki, L., 2010. Low intensity intra-epidermal electrical stimulation can activate A δ -nociceptors selectively. *Pain* 150, 199–207. doi:10.1016/j.pain.2010.04.026
- Mouraux, A., Iannetti, G.D., 2009. Nociceptive laser-evoked brain potentials do not reflect nociceptive-specific neural activity. *J. Neurophysiol.* 101, 3258–69. doi:10.1152/jn.91181.2008
- Oken, B.S., 1997. Endogenous event-related potentials, in: Chiappa, K.-H.- (Ed.), *Evoked Potentials in Clinical Medicine*. Lippincott-Raven Publishers, Philadelphia, pp. 529–563.
- Perchet, C., Frot, M., Charmarty, A., Flores, C., Mazza, S., Magnin, M., Garcia-Larrea, L., 2012. Do we activate specifically somatosensory thin fibres with the concentric planar electrode? A scalp and intracranial EEG study. *Pain* 153, 1244–1252. doi:10.1016/j.pain.2012.03.004
- Rattay, F., 1986. Analysis of models for external stimulation of axons. *IEEE Trans. Biomed. Eng.* BME-33, 974–977. doi:10.1109/TBME.1986.325670
- Treede, R.D., Lorenz, J., Baumgärtner, U., 2003. Clinical usefulness of laser-evoked potentials. *Neurophysiol. Clin.* 33, 303–314. doi:10.1016/j.neucli.2003.10.009
- Treede, R.D., Meyer, R.A., Raja, S.N., Campbell, J.N., 1995. Evidence for two different heat

transduction mechanisms in nociceptive primary afferents innervating monkey skin. *J Physiol* 483 (Pt 3, 747–758.

Acknowledgements: the authors are grateful to Prof. Claudia Spadavecchia, from the Vetsuisse Faculty, University of Bern, who spent her sabbatical at the laboratory of the Interuniversity Centre for Pain Neurophysiology and took part to some of the experiments.

Funding

This research did not receive any specific grant from funding agencies in the public, commercial, or not-for-profit sectors. All costs were covered by institutional funding from the Interuniversity Centre for Pain Neurophysiology (CIND) and the Physics Department of the University of Genova.

Declaration of Interest

The micropatterned 150 IDE is the object of a patent registration, joint property of the University of Genova and the Italian National Research Council (CNR). The authors M. Leandri, L. Pellegrino and A. Siri, as inventors, may receive a share of profits in case of commercialization and they declare a potential conflict of interest. L. Marinelli has no conflict of interest.

Highlights

- A new surface electrode for selective stimulation of nociceptive afferents is presented.
- The electrode is characterized by a micropattern with 150 μm gaps covering large areas without loss of selectivity.
- Only late SEP responses can be recorded with our electrode.
- Conversely, with a wider gap electrode, early and medium SEP components can be recorded.
- Lack of early and medium SEP components show selectivity of our electrode, which is an alternative to laser stimulation.